# Physicochemical aspects and cellular effects of nanoceria-human serum albumin conjugates

Elena V. Proskurnina $^{1,a}$ , Svetlana V. Kostyuk $^{1,2,b}$ , Madina M. Sozarukova $^{1,c}$ , Elizaveta S. Ershova $^{1,2,d}$ , Natalia N. Veiko $^{1,2,e}$ , Matvei A. Popkov $^{1,f}$ , Edmund V. Kostyuk $^{1,g}$ , Andrey V. Martynov $^{1,h}$ , Vladimir K. Ivanov $^{1,i}$ 

Corresponding author: E. V. Proskurnina, proskurnina@gmail.com

PACS 68.65.k, 81.20.n, 82.70.Dd, 87.68.+z

ABSTRACT Nanoceria exhibits unique catalytic properties towards reactive oxygen species (ROS), which act as mediators of key signaling pathways. Albumin is the most abundant blood protein, and its interaction with nanoceria modifies the properties of both nanoceria and albumin. Using an in vitro model of human embryonic lung fibroblasts, we investigated biochemical properties of nanoceria–albumin conjugates towards cell viability, intracellular reactive oxygen species, expression of NOX4, NRF2, and NF- $\kappa$ B, oxidative DNA damage/repair, apoptosis, cell proliferation, and autophagy. The results demonstrate that albumin binding alters the physicochemical properties of nanoceria, promoting efficient cellular uptake through modulation of surface interactions. This conjugation attenuates nanoceria's influence on intracellular reactive oxygen species equilibrium and mitochondrial membrane potential by modifying nanoparticle-protein interfacial dynamics. Notably, albumin-bound nanoceria induces a stronger activation of NOX4, resulting in increased genotoxic stress; however, the enhanced activation of DNA repair pathways mitigates this damage more efficiently than bare nanoceria. Furthermore, albumin-to-nanoceria conjugation modulates signaling pathways by enhancing suppression of the pro-inflammatory NF- $\kappa$ B cascade and stimulating autophagic processes. Overall, the physicochemical effects of nanoceria modification due to albumin conjugation reduce cytotoxicity of nanoceria while augmenting its anti-inflammatory and regenerative potential.

KEYWORDS nanoceria, human serum albumin, cytotoxicity, genotoxicity, oxidative metabolism genes, proliferation, autophagy, human lung embryonic fibroblasts.

ACKNOWLEDGEMENTS This study was supported by the Russian Science Foundation, project No. 24-13-00370.

FOR CITATION Proskurnina E.V., Kostyuk S.V., Sozarukova M.M., Ershova E.S., Veiko N.N., Popkov M.A., Kostyuk E.V., Martynov A.V., Ivanov V.K. Physicochemical aspects and cellular effects of nanoceria-human serum albumin conjugates. *Nanosystems: Phys. Chem. Math.*, 2025, **16** (5), 606–618.

## 1. Introduction

Nanoscale cerium dioxide (nanoceria) is a multifunctional catalyst for reactions involving reactive oxygen species (ROS). Acting as a nanozyme, nanoceria mimics the activities of enzymes such as superoxide dismutase (SOD) [1], peroxidase [2], catalase [3], oxidase [4,5], phosphatase [6], photolyase [7], phospholipase [8], and nuclease [9]. ROS play a central role in nearly all biological processes, positioning nanoceria as a key regulator of vital biochemical functions. Upon entry into biological fluids, nanoparticles interact primarily with proteins, altering the properties of both. Albumin, the predominant blood serum protein, exhibits high affinity for diverse compounds and contributes to redox balance via a single sulfhydryl group; its properties depend on its structural conformation [10]. Albumin functions as a transport protein and natural carrier within the organism, delivering drugs and metabolites [11], which ensures biocompatibility and strong binding characteristics when complexed with nanoparticles [12]. It is suitable as a drug delivery carrier due to its wide availability, low toxicity, biodegradability, non-immunogenicity, and preferential accumulation in tumors and inflamed tissues [13]. Conversely, when ceria nanoparticles enter the bloodstream, they bind to serum proteins,

<sup>&</sup>lt;sup>1</sup>Kurnakov Institute of General and Inorganic Chemistry of the Russian Academy of Sciences, Moscow 119991, Russia

<sup>&</sup>lt;sup>2</sup>Petrovsky Russian Scientific Center of Surgery, Institute of Longevity with a Clinic of Rehabilitation and Preventive Medicine, Moscow 119435, Russia

<sup>&</sup>lt;sup>a</sup>proskurnina@gmail.com, <sup>b</sup>svet-vk@yandex.ru, <sup>c</sup>s\_madinam@bk.ru,

<sup>&</sup>lt;sup>d</sup>es-ershova@rambler.ru, <sup>e</sup>satelit32006@yandex.ru, <sup>f</sup>ma\_popkov@igic.ras.ru,

gedmundvk@ya.ru, havlamar@mail.ru, van@igic.ras.ru

including albumin [14]. Therefore, albumin is actively studied for nanoparticle binding to develop effective anticancer nanomedicines and to elucidate their cellular mechanisms of action [12, 15].

Inorganic nanoparticles intended for biomedical applications require surface modification due to their low hydrophilicity and colloidal stability in solutions. Conjugation of the nanoparticles with albumin, which has high hydrophilicity, numerous binding sites, and reductive activity, facilitates effective functionalization [16, 17]. Compared to human serum albumin (HSA), bovine serum albumin (BSA) is rich in functional groups such as carboxyl and amino groups and exhibits strong affinity for inorganic (e.g. metal oxide) nanoparticles; therefore, it is often used as a model for surface modification of the nanoparticles to improve their colloidal stability and biocompatibility while providing functionalization and low toxicity [18, 19]. Most studies on conjugation of the nanoparticles with albumin focus on silver, gold, copper, and iron oxide. In particular, it has been shown that albumin conjugation reduced the cytotoxicity of silver nanoparticles on mesenchymal stem cells while preserving bactericidal activity [20]. HSA-coated silver nanoparticles showed higher toxicity toward hepatocellular carcinoma cells [21]. Chen *et al.* developed gold nanoparticle-albumin complexes conjugated with cisplatin, which exhibited reduced side effects [22]. Studies also report on albumin conjugation with copper particles [23] and magnetic iron oxides [24]. Janani *et al.* analyzed the toxicity of ZnO nanoparticles with BSA and demonstrated that BSA coating reduces the toxic effect [25].

The potential for forming nanocomplexes of cerium dioxide with albumin is also being investigated. Bhushan et al. reported the synthesis of albumin nanoparticles encapsulated with nanoceria, which constitute a highly monodisperse and stable aqueous delivery system. They demonstrated that the superoxide dismutase activity of nanoceria remained unaffected, and the nanoparticles exhibited high biocompatibility and antioxidant potential towards human lung epithelial cells [26]. Yang et al. synthesized ceria-based nanostructures – including nanoclusters, nanoparticles, and nanochains – using bovine serum albumin. The resulting albumin-based ceria nanostructures preserved high SOD-like activity and good biocompatibility [27]. Yeni et al. evaluated quercetin-albumin-nanoceria particles for neurotoxicity using the MTT assay on primary neuronal cultures and reported significant protective effects against glutamate toxicity [28]. Roudbaneh et al. examined the interaction of nano-CeO2 with human serum albumin (HSA), assessing antioxidant activity against peroxide-induced stress, bone marrow-derived mesenchymal stem cell viability, intracellular ROS, apoptosis, and antibacterial activity. Their findings indicated that hydrophilic interactions contribute to complex formation. No cytotoxicity was observed up to 50 mg/mL, and pre-treatment with this complex reduced cell death, ROS production, and apoptosis induced by peroxide stress. Cerium dioxide-albumin complex nanoparticles exerted significant antibacterial effects against all bacterial strains studied [29]. Although knowledge of the biological effects of the HSA-nanoceria complex remains limited and fragmented, it shows promising potential for biomedical applications. To date, no studies have addressed the effects of the HSA-nanoceria complex on human genes.

To summarize, complexation of nanoceria with human serum albumin (HSA) can be considered a promising approach for synthesizing new nanopharmacological agents. However, assessing the effects of surface modifiers on the efficacy and safety of cerium dioxide is essential to evaluate the benefits and risks in medical applications. Human embryonic lung fibroblasts serve as a widely used, reliable, and sensitive model for studying the effects of substances on gene expression. Here, we aimed to investigate the effects of the HSA-nanoceria conjugate on oxidative metabolism-related genes in human embryonic lung fibroblasts by examining: (1) cell viability and mitochondrial membrane potential, (2) intracellular reactive oxygen species (ROS), (3) expression levels of NOX4, NRF2, and NF- $\kappa$ B/STAT3, (4) oxidative DNA damage and repair, (5) cell proliferation, and autophagy.

#### 2. Materials and methods

#### 2.1. Synthesis and characterization of bare and HSA-nanoceria conjugate

The method for synthesizing an electrostatically stabilized  $CeO_2$  sol involved the thermal hydrolysis of ammonium cerium(IV) nitrate (Sigma-Aldrich, #215473) [30]. Specifically, a 100 g/L aqueous solution of  $(NH_4)_2Ce(NO_3)_6$  was incubated at 95°C for 24 hours. The product was centrifuged, washed three times with isopropanol, and then redispersed in deionized water. This suspension was boiled for 1 hour with stirring to remove residual isopropanol. In a separate preparation, albumin was dissolved in phosphate buffer. The HSA-CeO<sub>2</sub> conjugate was formed by the gradual, dropwise addition of the  $CeO_2$  sol to the albumin solution at a 1:1 molar ratio under constant stirring. The mixture was stirred for another 30 minutes after addition to complete albumin adsorption onto the  $CeO_2$  nanoparticles.

To determine the concentration of the stock  $CeO_2$  sol, a gravimetric method was employed. Sample aliquots were placed in pre-dried crucibles until constant weight was achieved. These samples were then evaporated and subjected to high-temperature treatment in a muffle furnace, held at  $900^{\circ}C$  for 4 hours.

X-ray diffraction (XRD) characterization of the dried samples was performed using a Bruker D8 Advance instrument (Bruker, Billerica, MA, USA) with  $CuK\alpha$  radiation. Data acquisition in  $\theta$ - $\theta$  geometry covered a  $2\theta$  range from 3° to  $120^{\circ}$ , with a step size of  $0.02^{\circ}$  and an accumulation time of 0.3 seconds per point. Phase identification via diffraction peak analysis was referenced to the ICDD PDF-2 database. The Scherrer equation was applied to calculate the mean crystallite size.

The mean hydrodynamic diameter of the  $CeO_2$  nanoparticles was measured by dynamic light scattering (DLS) using a Photocor Compact-Z analyzer (Photocor, Russia) with a 650 nm, 25 mW diode laser. Measurements were conducted at room temperature at a 90° scattering angle. Zeta potential was measured on a Malvern ZS Zetasizer (Malvern Panalytical, UK) according to the ISO/TR 19997:2018 standard. Both DLS and zeta potential analyses were carried out on aqueous nanoparticle dispersions at 1.5 mM concentration.

UV-Vis absorption spectra were recorded on a Cary 4000 spectrophotometer (Agilent Technologies, USA) using 1.0 cm path length quartz cuvettes at ambient temperature.

Binding affinity of ligand molecules to the cerium oxide nanoparticle surface was assessed by attenuated total reflectance-Fourier transform infrared spectroscopy (ATR-FTIR). Spectra were acquired using a Bruker VERTEX 70 spectrometer equipped with a PIKE Technologies GladiATR<sup>TM</sup> diamond crystal attachment. Measurements covered the wavenumber range  $4000-150~\text{cm}^{-1}$ , at 2 cm<sup>-1</sup> resolution, averaging 64 scans for both sample and background. The ATR crystal was maintained at  $50^{\circ}$ C. For liquid samples, up to 5  $\mu$ L were deposited onto the crystal and allowed to air-dry for 4-5 minutes before data acquisition.

## 2.2. Cell culture

Human embryonic lung fibroblasts (passage 4) were obtained from the Scientific Centre for Medical Genetics (Moscow, Russia). The cells were seeded at a concentration of  $1.7 \times 10^4$  cells/mL in Dulbecco's Modified Eagle Medium (PanEco, Moscow, Russia) supplemented with 10% fetal calf serum (PAA, Vienna, Austria), 50 U/mL penicillin, 50  $\mu$ g/mL streptomycin, and 10  $\mu$ g/mL gentamicin. HELFs were cultured at 37°C for 24 hours, followed by exposure to either bare nanoceria or the HSA-nanoceria conjugates for 1, 3, 24, and 72 hours.

## 2.3. Cell viability and mitochondrial potential

The standardized 72-hour MTT assay (3-(4,5-dimethylthiazol-2-yl)-2,5-diphenyltetrazolium bromide) was employed to assess cell viability. Absorbance at 550 nm was measured using an EnSpire Plate Reader (EnSpire Equipment, Turku, Finland). Cells incubated without nanoparticles served as the negative control. Mitochondrial membrane potential was evaluated using the membrane-potential-sensitive dye tetramethylrhodamine methyl ester (TMRM) (Thermo Fisher, Waltham, MA, USA), following previously established protocols [31].

#### 2.4. Visualization

An AxioImagerA2 microscope (Carl Zeiss, Oberkochen, Germany) was used for fluorescence imaging. Cells were cultured in slide flasks and exposed to either bare or HSA-bound nanoceria. Each slide-bottom flask was seeded with approximately 500,000 cells. Following medium removal, the cells were washed with phosphate buffered saline (PBS), and dichlorodihydrofluorescein diacetate (a 2 mg/mL stock solution diluted 1:200 with PBS) was added. After a 15-minute incubation, the cells were washed once more with PBS and immediately imaged. At least 100 fields of view were analyzed. Fluorescence intensity per cell and total fluorescence were quantified using the microscope software (ZEN 3.10).

# 2.5. Flow cytometry analysis

Intracellular reactive oxygen species (ROS) and protein expression were quantified using flow cytometry. To measure ROS, samples were incubated with a 10  $\mu$ M solution of 2',7'-dichlorodihydrofluorescein diacetate (H2DCFH-DA) in phosphate-buffered saline (PBS) (Molecular Probes/Invitrogen, Carlsbad, CA, USA) for 15 minutes in the dark. Following incubation, the cells were washed with PBS, resuspended in PBS, and analyzed by flow cytometry using the FITC channel (CytoFlex S, Beckman Coulter, Brea, CA, USA).

For protein quantification, cells were washed with Versene solution (Thermo Fisher Scientific, Waltham, MA, USA), treated with 0.25% trypsin (Paneco, Moscow, Russia), washed with culture medium, and then resuspended in PBS (pH 7.4) (Paneco, Moscow, Russia). The cells were fixed with paraformaldehyde (PFA, Sigma-Aldrich, Saint Louis, MO, USA) at  $37^{\circ}$ C for 10 minutes, washed three times with 0.5% bovine serum albumin (BSA) in PBS, and permeabilized with either 0.1% Triton X-100 in PBS for 15 minutes at  $20^{\circ}$ C or 90% methanol at  $4^{\circ}$ C. After three washes with 0.5% BSA-PBS, cells were stained with conjugated antibodies (1  $\mu$ g/mL) for 2 hours at room temperature, washed with PBS, and analyzed by flow cytometry (CytoFlex S, Beckman Coulter, Brea, CA, USA).

Primary antibodies were as follows: DyLight488-γH2AX (pSer139) (nb100-78356G, NovusBio, Centennial, CO, USA), FITC-NRF2, (bs1074r-fitc, Bioss Antibodies Inc. Woburn, MA, USA), FITC-BRCA1 (Nb100-598F, NovusBio, Centennial, CO, USA), PE-8-oxo-dG (sc-393871 PE, Santa Cruz Biotechnology, Dallas, TX, USA), CY5.5-NOX4 (bs-1091r-cy5-5, Bioss Antibodies Inc. Woburn, MA, USA), A350-BCL2 (bs-15533r-a350, Bioss Antibodies Inc. Woburn, MA, USA), NFKB (bs-0465r-cy7, Bioss Antibodies Inc. Woburn, MA, USA), LC3 (NB100-2220 NovusBio, Centennial, CO, USA), and PCNA (ab2426, Abcam plc, Cambridge, UK). The secondary anti-rabbit IgG-FITC (sc-2359, Santa Cruz Biotechnology, Dallas, TX, USA), was used.

Sample	Particle Size, nm	Particle Size, nm	$\zeta$ , mV
	(Powder X-Ray Diffraction)	(Dynamic Light Scattering)	(Electrophoretic Light Scattering)
Bare CeO <sub>2</sub>	$3.2 \pm 0.3$	$20.7 \pm 0.3$	$+40.2 \pm 0.1$
HSA-			
nanoceria	$3.9 \pm 0.1$	$9.2 \pm 0.1, 180 \pm 11$	$+9.8\pm1.2$
conjugate			

TABLE 1. Physicochemical characteristics of CeO<sub>2</sub> sols

#### 2.6. Statistics

All experiments were performed in triplicate. Data are presented as the mean  $\pm$  standard deviation. Differences were considered statistically significant at p < 0.01 according to the non-parametric Mann–Whitney test. Statistical analyses were conducted using StatPlus2007 Pro v4.9.2 software (AnalystSoft Inc., Walnut, CA, USA).

#### 3. Results

#### 3.1. Synthesis and characterization of nanoparticles

An electrostatically stabilized cerium dioxide sol was synthesized from ammonium cerium(IV) nitrate via thermal hydrolysis at  $95^{\circ}$ C [30]. The concentration of the  $CeO_2$  colloidal dispersion, determined by thermogravimetric analysis, was  $0.125 \pm 0.003$  mol/L (21.5 g/L). Crystallite sizes and zeta potential values of bare  $CeO_2$  nanoparticles and the HSA-nanoceria conjugate, measured by powder X-ray diffraction (XRD), dynamic light scattering (DLS), and electrophoretic light scattering (ELS), are summarized in Table 1.

The XRD patterns of the ceria sols, both dried at a low temperature  $(50^{\circ}\text{C})$ , are shown in Fig. 1. According to experimental data, powder samples contain single-phase fluorite-type cerium dioxide (PDF2 34-0394) with crystallite sizes in the range of 3.2 - 3.9 nm (Table 1). The XRD pattern of the HSA-nanoceria conjugate is similar to that of bare CeO<sub>2</sub> NPs, indicating that the crystalline structure of nanoscale cerium dioxide is retained after interaction with albumin.

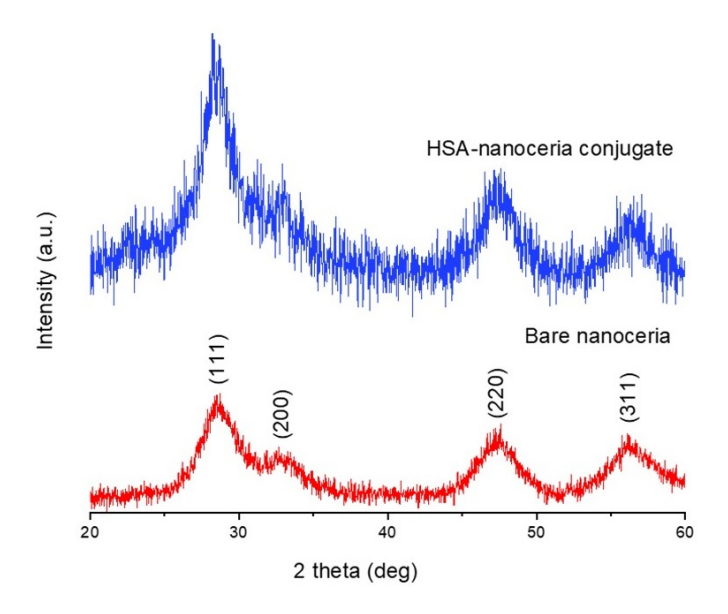


FIG. 1. XRD patterns of the dried sols of bare and HSA-coated CeO<sub>2</sub>

Dynamic light scattering data on the particle size distribution of aggregates in  $CeO_2$  sols are shown in Fig. 2. The non-stabilized  $CeO_2$  sol (pH $\sim$ 3.0) exhibits a nearly monomodal size distribution of aggregates with an average hydrodynamic diameter of 20 nm (Table 1). The conjugation of albumin to  $CeO_2$  nanoparticles (NPs) alters their degree of aggregation, resulting in larger aggregates with an average hydrodynamic diameter of 180 nm (Table 1). The small-size particles ( $\sim$ 10 nm) that are present in the HSA-nanoceria conjugate dispersions are most probably the individual HSA moieties. The HSA characteristic size in different water solutions (5 – 30 nm) has been extensively studied earlier and corresponds well to the observed value [32–34]. These data indicate that not all the HSA was conjugated with ceria nanoparticles, however the relative amount of the free protein could be regarded as low.

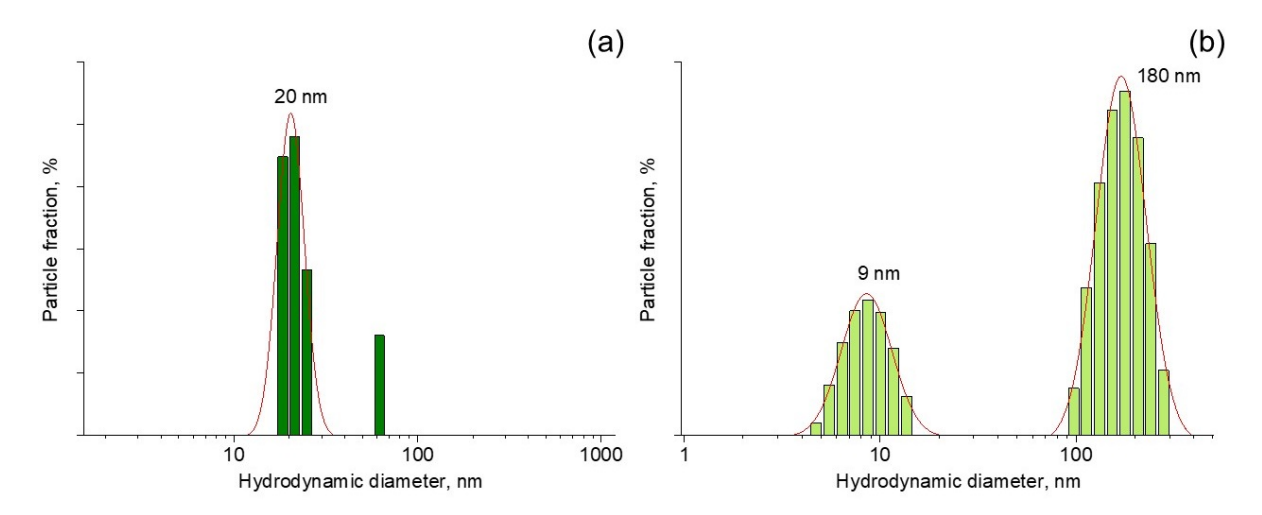


FIG. 2. Hydrodynamic diameters distributions for CeO<sub>2</sub> particles in aqueous sols (a) non-stabilized ceria sol and (b) HSA-nanoceria conjugate

According to the results of electrokinetic measurements (Table 1), the zeta potential of bare  $CeO_2$  nanoparticles is  $+40.2\pm0.1$  mV, indicating their high colloidal stability. As the non-stabilized  $CeO_2$  sol has a pH of approximately 3.0, the positive surface charge is attributed to protonation of surface hydroxyl groups [35, 36]. Modification of the  $CeO_2$  nanoparticles with albumin causes a sharp decrease in zeta potential to  $+9.8\pm1.2$  mV. This decrease is consistent with protein adsorption onto the nanoparticle surface and the formation of a dense protein corona [37–39].

UV-vis absorption spectroscopy data (Fig. 3) show an absorption band in the 280 - 300 nm wavelength range. This band is characteristic of nanoscale cerium dioxide and corresponds to a band gap of  $\sim 3.4$  eV, which is consistent with values reported in the literature [40].

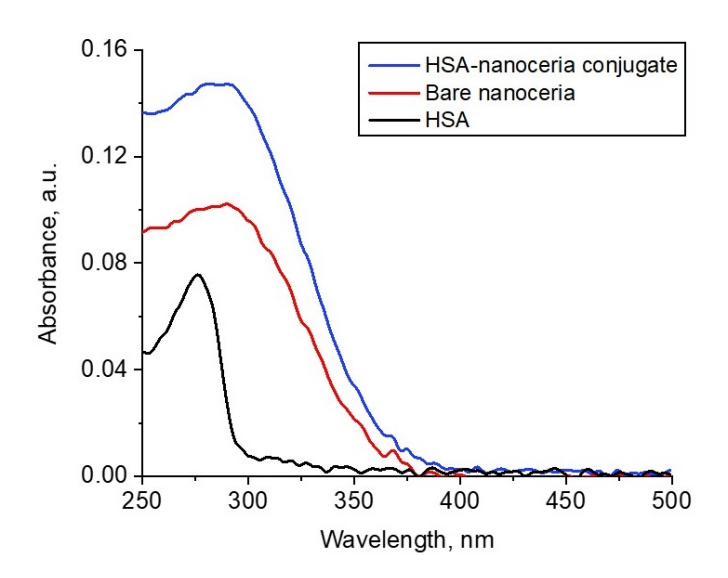


FIG. 3. UV-vis absorption spectra of ceria sols

The ceria sols were characterized using ATR-FTIR spectroscopy. The FTIR spectra of bare CeO<sub>2</sub> nanoparticles, human serum albumin, and the HSA-nanoceria conjugate are presented in Fig. 4.

The FTIR spectrum of the bare CeO<sub>2</sub> nanoparticles features characteristic absorption bands for Ce–O valence vibrations at 470 cm<sup>-1</sup> and 285 cm<sup>-1</sup>. Additional bands observed in the regions of 1600 – 1395 cm<sup>-1</sup> and 3500 cm<sup>-1</sup> are assigned to deformation and valence vibrations of water adsorbed on the ceria surface [41]. The absorption band at 1288 cm<sup>-1</sup> corresponds to residual nitrate ions from the synthesis precursor, ammonium cerium(IV) nitrate ((NH<sub>4</sub>)<sub>2</sub>Ce(NO<sub>3</sub>)<sub>6</sub>) [42]. The absorption bands of the native HSA (Fig. 4) are consistent with those previously reported [43,44]. The Amide I band, arising from C=O stretching vibrations, is located at 1655 cm<sup>-1</sup>. The amide II band, which is attributed to C–N stretching coupled with N–H bending modes, appears at 1542 cm<sup>-1</sup>. These bands are sensitive to changes in the secondary structure of the protein [43–45]. Presumably, the bands at 1085 cm<sup>-1</sup> and 982 cm<sup>-1</sup> are due to the phosphate buffer used to prepare the protein solution. The intense band at 530 cm<sup>-1</sup> is due to the stretching vibrations of the S–S bonds of the

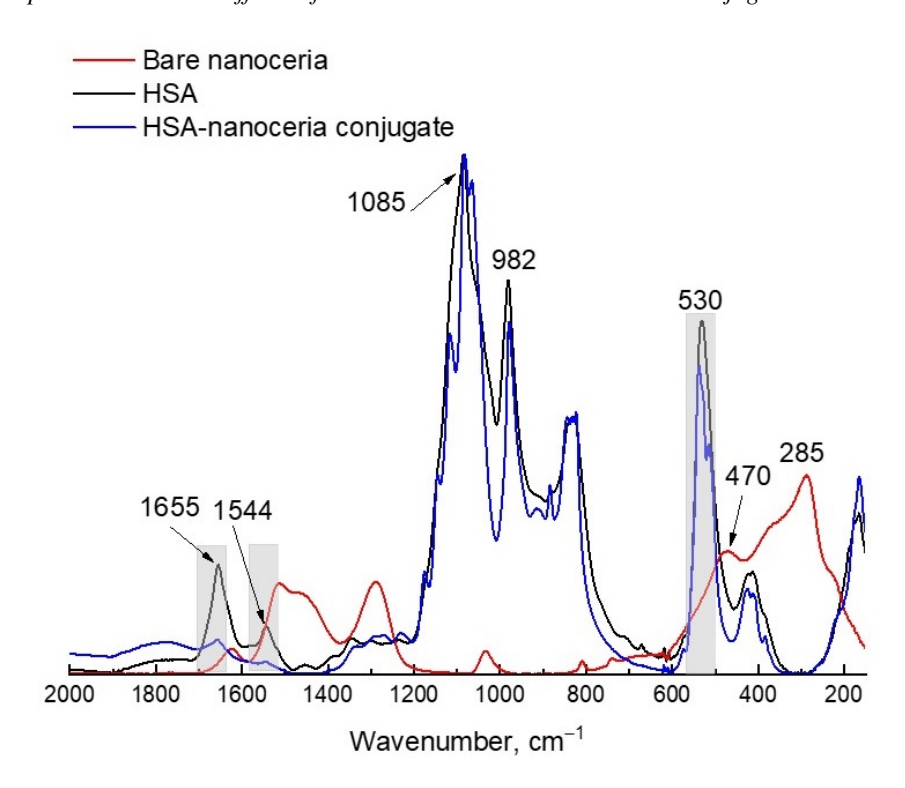


FIG. 4. Fourier-transform infrared spectra with attenuated total reflection for bare CeO<sub>2</sub>, human serum albumin (HSA), and HSA-nanoceria conjugate

disulfide bridges present in human serum albumin [46]. The FTIR spectrum of the conjugate (Fig. 4) reveals a significant reduction in intensity and broadening of the amide I and II bands at  $\sim$ 1655 cm<sup>-1</sup> and at  $\sim$ 1540 cm<sup>-1</sup>, alongside a shift of the S–S band from 530 cm<sup>-1</sup> to 540 cm<sup>-1</sup>. All this indicates conformational changes in the protein structure as a result of interaction with CeO<sub>2</sub> nanoparticles. The shift in the disulfide bond vibration band may suggest that the nanoparticles interact with albumin domains containing cysteine residues [47]. These results confirm the successful formation of the conjugate and extend the previous findings on the interaction of nanoceria with proteins [37].

## 3.2. Cell viability and mitochondrial potential

Viability of cells exposed to bare nanoceria and HSA-nanoceria conjugate shows a similar pattern (Fig. 5a). There is a slight increase in toxicity around the concentration of 1  $\mu$ mol/L, whereas nanoceria conjugated with albumin is also more toxic at higher concentrations (above 85  $\mu$ mol/L). For gene and protein expression studies, a concentration of 1.5  $\mu$ mol/L was selected, corresponding to the middle of the investigated range and providing satisfactory viability for both bare nanoceria and HSA-conjugated nanoceria.

Regarding mitochondrial membrane potential, the HSA-nanoceria conjugate exhibits a milder effect compared to bare nanoceria (Fig. 5b), although the maximum increase in membrane potential for both nanoparticles occurs after 3 hours of incubation. After 24 hours of incubation, the membrane potential returns to control levels.

# 3.3. Visualization and intracellular ROS

Nanoscale cerium dioxide yields fluorescence in the red region, enabling visualization of its accumulation within cells [48]. Images of cells exposed to nanoparticles (1.5  $\mu$ mol/L) for 3 hours are presented in Fig. 6. The images indicate that during the first three hours, the HSA-nanoceria conjugate actively enters the cells.

Assessment of intracellular ROS levels using flow cytometry and H2DCFH-DA indicates that bare nanoceria exhibits an antioxidant effect during 1 and 3 hours of incubation, whereas albumin-bound nanoceria has little to no impact on intracellular ROS levels (Fig. 7).

# 3.4. Genotoxicity

Genotoxicity was evaluated using the oxidative damage marker 8-oxo-2'-deoxyguanosine (8-oxo-dG) (Fig. 8a) and the marker of double-strand breaks, phosphorylated histone  $\gamma$ H2AX (Fig. 8b). Repair system activity was assessed by the key repair protein marker BRCA1 (Fig. 8c).

The genotoxicity dynamics differ slightly for bare nanoceria and HSA-nanoceria conjugate, with a peak at 3 hours of incubation. Bare nanoceria exhibits two phases of action, with peaks at 1 and 24 hours, while the peak effect for HSA-albumin conjugate is 3 hours. HSA-nanoceria conjugate is also characterized by higher levels of DNA damage and

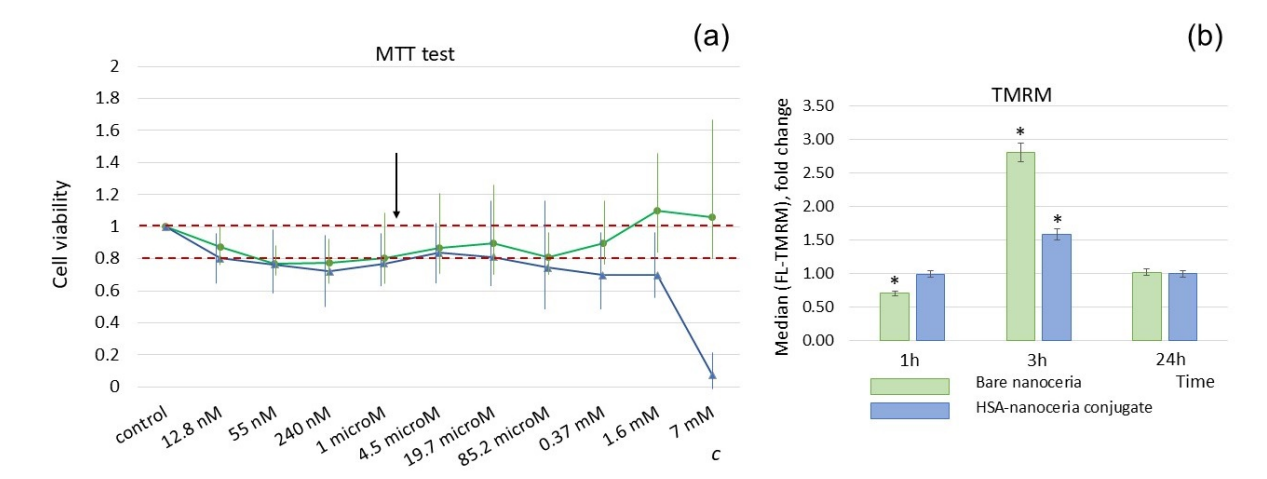


FIG. 5. (a) Cell viability in the presence of bare nanoceria (green line) and HSA-nanoceria conjugate (blue line), assessed by the MTT assay. The red dashed line indicates the acceptable viability range of 80-100 %. The arrow points to the concentration of 1.5  $\mu$ mol/L selected for further studies; (b) Mitochondrial membrane potential relative to control, measured by the TMRM assay for cells exposed to bare and HSA-nanoceria conjugate; asterisks (\*) indicate significant differences from the control according to the Mann–Whitney test (p < 0.05). The control consists of cells incubated without nanoparticles

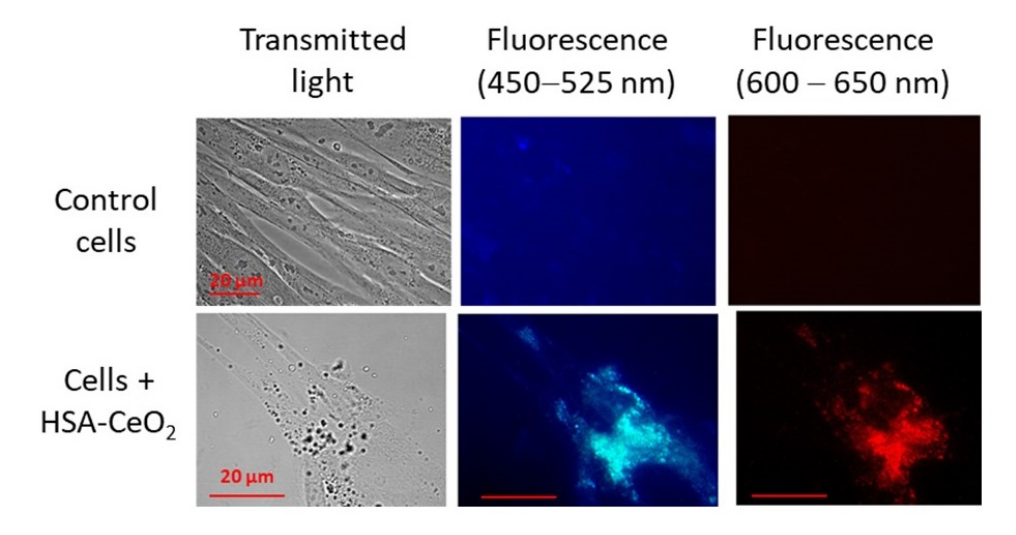


FIG. 6. Transmitted light and fluorescence images of HSA-nanoceria conjugate (1.5  $\mu$ M) in human fetal lung fibroblasts; magnification,  $100\times$ 

repair. After 72 hours of incubation, the level of DNA damage for both nanoparticles decreases significantly below the control level, with this effect being more pronounced for HSA-albumin conjugate.

# 3.5. Proteins of key ROS-dependent and inflammation signaling pathways

The primary prooxidant enzyme is the membrane-bound complex NOX4, whose expression is highest following 3 hours of incubation with the HSA-nanoceria conjugate (Fig. 9a). This correlates with the compensatory activation of the NRF2 anti-inflammatory pathway (Fig. 9b). The expression dynamics of NOX4 and NRF2 correspond to the patterns of oxidative DNA damage observed for both nanoparticles (compare Fig. 8a,b and Fig. 9a,b). The effects are more pronounced for the HSA-nanoceria conjugate than for bare nanoceria.

Regarding the pro-inflammatory NF- $\kappa$ B pathway, the HSA-nanoceria conjugate activated it only slightly after 24 hours of incubation, in contrast to the more pronounced effect of bare nanoceria (Fig. 9c). For the STAT3 pathway, the activating effect of both nanoparticles peaked after 3 hours of incubation and was virtually identical (Fig. 9d).

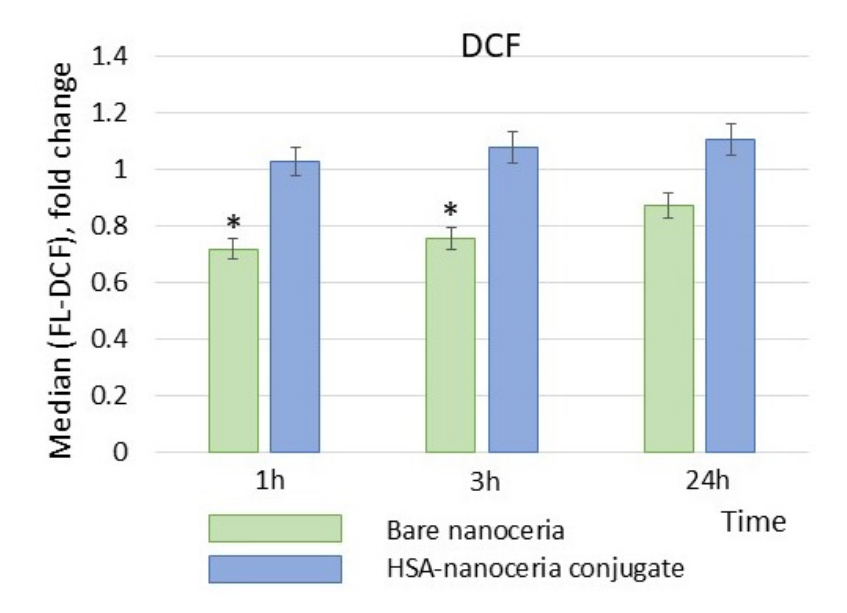


FIG. 7. Levels of intracellular reactive oxygen species (ROS), assessed by oxidation of the fluorescent probe H2DCFH-DA using flow cytometry. Incubation times with nanoparticles (1.5  $\mu$ mol/L) are indicated in the figure. Results are shown relative to control cells incubated without nanoparticles; asterisks (\*) denote significant differences according to the Mann–Whitney test (p < 0.05)

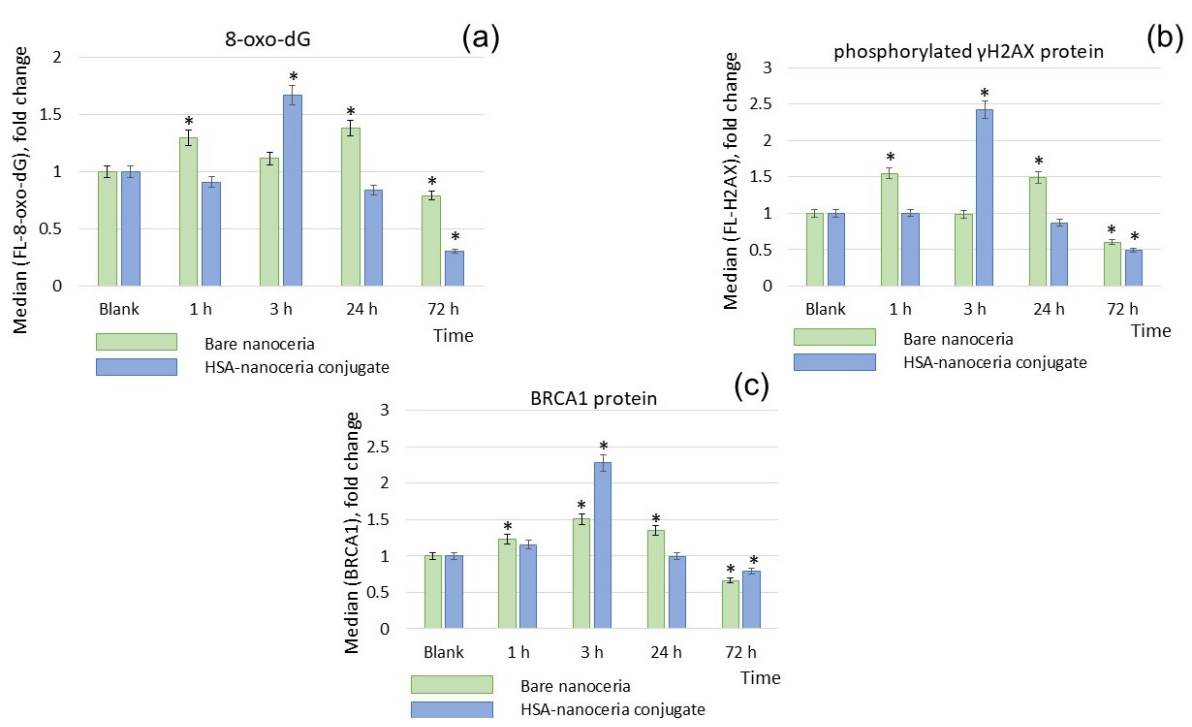


FIG. 8. (a) Levels of the DNA oxidative damage marker 8-oxo-2'-deoxyguanosine (8-oxo-dG), (b) levels of the DNA double-strand break marker phosphorylated histone  $\gamma$ H2AX, and (c) expression levels of the DNA repair marker protein BRCA1; cells were incubated with bare and HSA-nanoceria conjugate (1.5  $\mu$ mol/L) for 1 – 72 hours. Results are presented relative to control cells incubated without nanoparticles; asterisks (\*) indicate significant differences according to the Mann–Whitney test (p < 0.05)

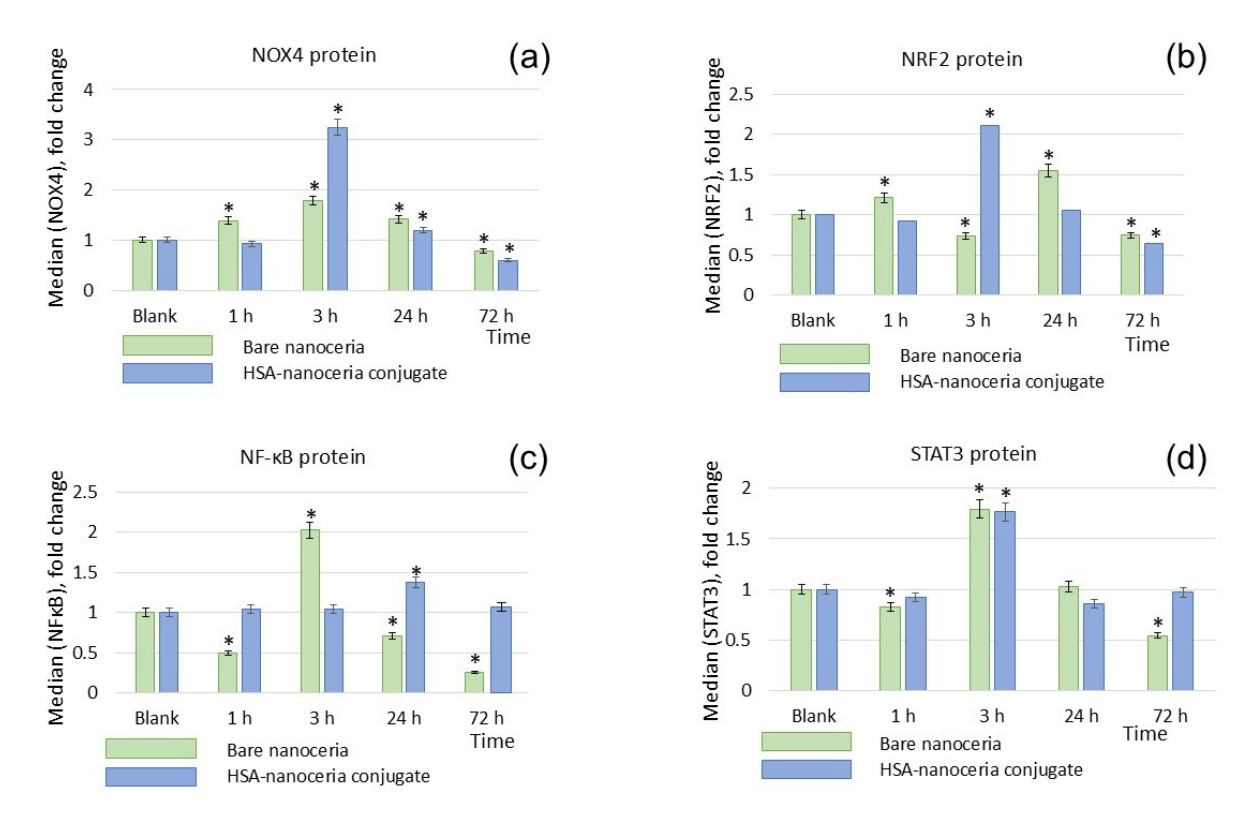


FIG. 9. Protein expression levels of (a) NOX4, (b) NRF2, (c) NF- $\kappa$ B, and (d) STAT3 in cells; data are presented relative to control cells incubated without nanoparticles. Asterisks (\*) indicate significant differences according to the Mann–Whitney test (p < 0.05)

# 3.6. Proteins of proliferation and autophagy

Regarding the pro-inflammatory NF- $\kappa$ B pathway, the HSA-nanoceria conjugate activates it to a lesser extent after 24 hours of incubation, unlike the more pronounced effect of bare nanoceria (Fig. 10). For the STAT3 pathway, the activating effect of both nanoparticles is maximal at 3 hours of incubation and is practically the same.

## 4. Discussion

Nanoceria can be considered a promising nanopharmacological agent due to its regenerative and proliferative effects on normal cells and its cytotoxicity toward cancer cells. Therefore, the development of new pharmacological formulations, particularly those involving surface-modifying agents, is of great importance. The roles of surface modifiers vary depending on their chemical properties. The objectives of modification include stabilizing the colloidal system, facilitating nanoparticle cellular uptake, reducing toxicity, and enhancing the targeted therapeutic efficacy of nanoparticles. Multifunctional nanoparticle synthesis strategies enable the creation of novel therapeutic platforms for targeted cell therapy. In this study, we investigated albumin as a modifier of nanoceria properties and compared the resulting data with those of bare nanoceria.

The main findings for the HSA-nanoceria conjugate in this study are as follows: (1) HSA-nanoceria conjugate, like bare nanoceria, actively penetrates cells during the first three hours, indicating that albumin binding ensures effective cellular internalization within this timeframe; (2) unlike bare nanoceria, HSA-nanoceria conjugate does not alter intracellular ROS balance and has a less pronounced effect on mitochondrial membrane potential; (3) compared to bare nanoceria, HSA-nanoceria conjugate induces a more pronounced activation of NOX4 within 3 hours, resulting in greater genotoxicity (oxidative DNA damage and double-strand breaks); however, it also triggers stronger activation of DNA repair systems, leading to more effective neutralization of NOX4 activity and its effects after 72 hours; (4) no differences were observed between HSA-nanoceria conjugate and bare nanoceria in terms of proliferative properties and activation of the STAT3 cytokine pathway; (5) the HSA-nanoceria conjugate exhibits a pronounced suppressive effect on the proinflammatory NF- $\kappa$ B pathway after 72 hours; (6) the conjugate increases the level of the autophagy marker LC3.

Interestingly, HSA-nanoceria conjugate does not alter intracellular ROS levels, unlike bare nanoceria, which exhibits valuable redox activity properties. However, the HSA-nanoceria conjugate activates NOX4 approximately twice as strongly, leading to enhanced activation of NRF2, increased oxidative DNA damage, and stimulation of repair mechanisms. Albumin conjugation does not affect nanoceria's influence on the STAT3 cytokine pathway or cell proliferation. Regarding the NF- $\kappa$ B pathway, both bare and albumin-bound nanoceria initially activate and subsequently significantly

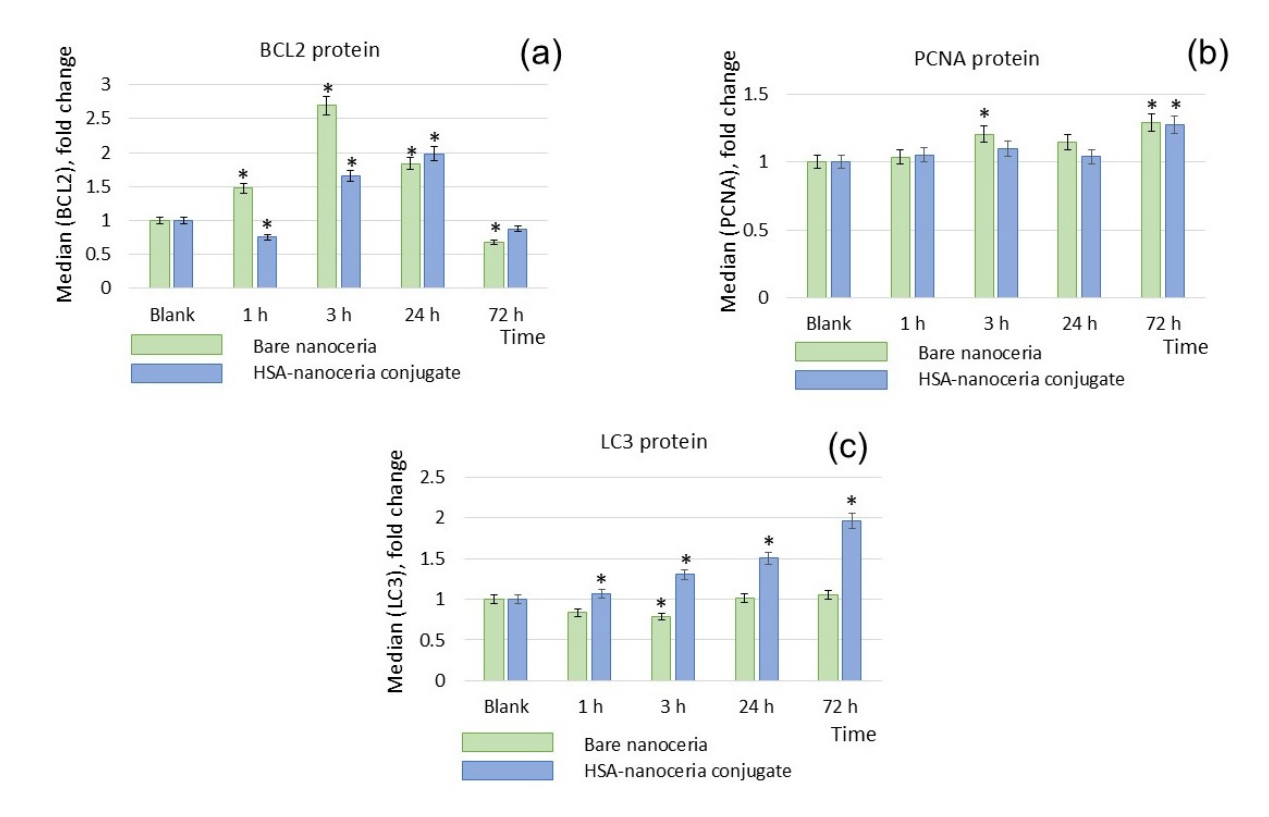


FIG. 10. Expression levels of proliferation proteins (a) PCNA, (b) BCL2, and (c) the autophagy protein LC3; data are presented relative to control cells incubated without nanoparticles; asterisks (\*) indicate significant differences according to the Mann–Whitney test (p < 0.05)

suppress it. For bare nanoceria, NF- $\kappa$ B activation peaks at 3 hours, whereas for HSA-nanoceria conjugate, the peak occurs at 24 hours. Ultimately, after 72 hours, NF- $\kappa$ B activity decreases threefold with bare nanoceria and nearly to zero with HSA-nanoceria conjugate. Thus, HSA-nanoceria conjugate demonstrates a pronounced anti-inflammatory effect after prolonged incubation.

Studies on the interaction between bovine serum albumin and nanoceria confirm the formation of a BSA-nanoceria complex mediated by electrostatic interactions and accompanied by conformational changes in the protein [45, 49]. Liu *et al.* demonstrated that, for nanoparticles interacting with proteins of comparable size, a heteroaggregate model is more appropriate than the conventional protein corona concept. They showed that in heteroaggregates of nanoceria with BSA, the surface properties of the nanoparticles remain unchanged, while the protein structure undergoes alteration [50]. The unique spatial and redox characteristics of bovine serum albumin have been exploited for the targeted synthesis of cerium dioxide nanoparticles exhibiting effective nanozyme properties [27], highlighting the strong mutual influence between the protein and cerium dioxide nanoparticles. Albumin nanoparticles encapsulating cerium dioxide have been proposed as stable aqueous systems with potent nanozyme activities, and their biocompatibility has been demonstrated in vitro using human lung epithelial cell cultures [26].

Similar findings have been reported for human serum albumin. Butterfield *et al.* conducted proteomic analyses to identify plasma and serum proteins adsorbed onto nanoceria. They concluded that the protein corona can either enhance or inhibit cellular uptake of nanoceria and modulate subsequent biological effects. Moreover, interactions with nanoceria can induce structural and functional changes in proteins, including pro- and anti-inflammatory effects. The authors emphasize the need for a deeper understanding of nanoparticle-protein interactions prior to the therapeutic application of nanoceria [14]. Simon-Vazquez *et al.* demonstrated that HSA interaction with nanoceria leads to conformational changes predominantly involving the conversion of alpha-helices into beta-sheet structures, with these effects being pH-dependent [50]. We have previously confirmed the formation of HSA-nanoceria conjugates, noting that the transport function of HSA remains unaffected [37].

Although the molecular mechanisms of interaction between nanoceria and albumin have been well studied [29,45,49–51], few studies have addressed the biological activity of the albumin-nanoceria complex. Yang *et al.* demonstrated that nanoceria retains superoxide dismutase (SOD)-like properties [27]. Of particular interest is the study by Yeni *et al.*, who investigated the effects of quercetin-albumin-nanoceria triple nanoparticles on glutamate-induced neurotoxicity in an in vitro model [28]. Cytotoxicity was assessed using the MTT assay, along with oxidative stress parameters including lactate dehydrogenase, total oxidative status, total antioxidant capacity, and reduced glutathione. Treatment of glutamate-injured cells with these nanoparticles significantly enhanced cell survival and improved oxidative stress markers.

On the other hand, binding to nanoparticles can alter the properties of albumin [14] since the properties of albumin depend on its structure [10], and binding induces conformational changes. As nanoceria and albumin are antioxidants with different mechanisms of action – nanoceria exhibits nanozyme activity against reactive oxygen species, while albumin is a thiol-based antioxidant – it is important to study their mutual influence on each other's oxidative properties. Previously, we investigated the antioxidant activity of cerium dioxide nanoparticle conjugates [52] and showed that the interaction of CeO<sub>2</sub> nanoparticles with purified human serum albumin results in an approximately 1.5-fold decrease in both the antioxidant and prooxidant potential of albumin. This is presumably caused by the interaction of nanoscale CeO<sub>2</sub> with the sulfhydryl groups of the protein. We also studied the transport function of albumin upon interaction with nanoceria and confirmed the formation of HSA-CeO<sub>2</sub> nanoparticle conjugates. Changes in protein conformation did not affect albumin's drug-binding sites and, accordingly, did not impair HSA's transport function [37]. In the same study, we demonstrated that a 1:1 molar ratio of protein to nanoscale CeO<sub>2</sub> forms a conjugate, whereas at higher protein ratios, a protein corona forms around the nanoparticle.

#### 5. Conclusions

Using an *in vitro* model of human embryonic lung fibroblasts, this study highlights the significant influence of albumin conjugation on the physicochemical behavior of nanoceria over prolonged incubation (72 hours). The albumin coating modulates the surface charge and colloidal stability of nanoceria, which in turn attenuates its impact on intracellular redox processes and mitochondrial membrane potential. The altered nanoparticle-protein interface facilitates enhanced control over reactive oxygen species dynamics, leading to more efficient suppression of pro-inflammatory signaling and oxidative DNA damage. Additionally, the conjugation promotes autophagic responses, reflecting a physicochemically driven modulation of cellular pathways. These findings underscore the importance of nanoparticle surface chemistry and protein interactions in tuning the bioactivity of cerium dioxide, supporting its potential as an anti-inflammatory and regenerative nanomaterial.

#### References

- [1] Korsvik C., Patil S., Seal S. et al. Superoxide dismutase mimetic properties exhibited by vacancy engineered ceria nanoparticles. *Chem. Commun.*, 2007. **10**. P. 1056.
- [2] Ivanov V.K., Usatenko A.V., Shcherbakov A.B. Antioxidant activity of nanocrystalline ceria to anthocyanins. *Russ. J. Inorg. Chem.*, 2009, **54**(10), P. 1522–1527.
- [3] Pirmohamed T., Dowding J.M., Singh S. et al. Nanoceria exhibit redox state-dependent catalase mimetic activity. *Chem. Commun.*, 2010, **46**(16), P. 2736.
- [4] Asati A., Santra S., Kaittanis C. et al. Oxidase-Like Activity of Polymer-Coated Cerium Oxide Nanoparticles. *Angew. Chemie Int. Ed.*, 2009, 48(13), P. 2308–2312.
- [5] Liu B., Huang Z., Liu J. Boosting the oxidase mimicking activity of nanoceria by fluoride capping: rivaling protein enzymes and ultrasensitive F<sup>-</sup> detection. *Nanoscale*, 2016, **8**(28), P. 13562–13567.
- [6] Yao T., Tian Z., Zhang Y. et al. Phosphatase-like Activity of Porous Nanorods of CeO<sub>2</sub> for the Highly Stabilized Dephosphorylation under Interferences. ACS Appl. Mater. Interfaces, 2019, 11(1), P. 195–201.
- [7] Tian Z., Yao T., Qu C. et al. Photolyase-Like Catalytic Behavior of CeO<sub>2</sub>. Nano Lett., 2019, 19(11), P. 8270–8277.
- [8] Khulbe K., Karmakar K., Ghosh S. et al. Nanoceria-Based Phospholipase-Mimetic Cell Membrane Disruptive Antibiofilm Agents. ACS Appl. Bio Mater., 2020, 3(7), P. 4316–4328.
- [9] Xu F., Lu Q., Huang P.-J.J. et al. Nanoceria as a DNase I mimicking nanozyme. Chem. Commun., 2019, 55(88), P. 13215–13218.
- [10] Wu N., Liu T., Tian M. et al. Albumin, an interesting and functionally diverse protein, varies from 'native' to 'effective' (Review). *Mol. Med. Rep.*, 2023, **29**(2), P. 24.
- [11] Tao C., Chuah Y.J., Xu C. et al. Albumin conjugates and assemblies as versatile bio-functional additives and carriers for biomedical applications. J. Mater. Chem. B. 2019, 7(3), P. 357–367.
- [12] Qu N., Song K., Ji Y. et al. Albumin Nanoparticle-Based Drug Delivery Systems. Int. J. Nanomedicine, 2024, 19, P. 6945–6980.
- [13] Tincu C.-E., Andritoiu C.V., Popa M. et al. Recent Advancements and Strategies for Overcoming the Blood–Brain Barrier Using Albumin-Based Drug Delivery Systems to Treat Brain Cancer, with a Focus on Glioblastoma. *Polymers* (Basel), 2023, **15**(19), P. 3969.
- [14] Butterfield A.D., Wang B., Wu P. et al. Plasma and Serum Proteins Bound to Nanoceria: Insights into Pathways by which Nanoceria may Exert Its Beneficial and Deleterious Effects In Vivo. *J. Nanomed. Nanotechnol.*, 2020, 11(4), P. 546.
- [15] Fanciullino R., Ciccolini J., Milano G. Challenges, expectations and limits for nanoparticles-based therapeutics in cancer: A focus on nano-albumin-bound drugs. Crit. Rev. Oncol. Hematol., 2013, 88(3), P. 504–513.
- [16] Zhu Y., Xue J., Chen W. et al. Albumin-biomineralized nanoparticles to synergize phototherapy and immunotherapy against melanoma. J. Control. Release, 2020, 322, P. 300–311.
- [17] Gou Y., Zhang Z., Qi J. et al. Folate-functionalized human serum albumin carrier for anticancer copper(II) complexes derived from natural plumbagin. *J. Inorg. Biochem.*, 2015, **153**, P. 13–22.
- [18] Kim D., Amatya R., Hwang S. et al. BSA-Silver Nanoparticles: A Potential Multimodal Therapeutics for Conventional and Photothermal Treatment of Skin Cancer. *Pharmaceutics*, 2021, **13**(4), P. 575.
- [19] Jaiswal V.D., Pangam D.S., Dongre P.M. Biophysical study of cisplatin loaded albumin-gold nanoparticle and its interaction with glycans of gp60 receptor. *Int. J. Biol. Macromol.*, 2023, **231**, P. 123368.
- [20] Korolev D., Shumilo M., Shulmeyster G. et al. Hemolytic Activity, Cytotoxicity, and Antimicrobial Effects of Human Albumin- and Polysorbate-80-Coated Silver Nanoparticles. Nanomaterials, 2021, 11(6), P. 1484.
- [21] Park H.-Y., Chung C., Eiken M.K. et al. Silver nanoparticle interactions with glycated and non-glycated human serum albumin mediate toxicity. *Front. Toxicol.*, 2023, **5**, P. 1081753.

- [22] Chen J.L.-Y., Yang S.-J., Pan C.-K. et al. Cisplatin and Albumin-Based Gold-Cisplatin Nanoparticles Enhance Ablative Radiation Therapy— Induced Antitumor Immunity in Local and Distant Tumor Microenvironment. Int. J. Radiat. Oncol., 2023, 116(5), P. 1135–1149.
- [23] Gou Y., Zhang Y., Qi J. et al. Enhancing the copper(II) complexes cytotoxicity to cancer cells through bound to human serum albumin. J. Inorg. Biochem., 2015, 144, P. 47–55.
- [24] He C., Xie M., Hong F. et al. A Highly Sensitive Glucose Biosensor Based on Gold Nanoparticles/Bovine Serum Albumin/Fe<sub>3</sub>O<sub>4</sub> Biocomposite Nanoparticles. *Electrochim. Acta*, 2016, 222, P. 1709–1715.
- [25] Janani B., Raju L.L., Thomas A.M. et al. Impact of bovine serum albumin A protein corona on toxicity of ZnO NPs in environmental model systems of plant, bacteria, algae and crustaceans. *Chemosphere*, 2021, **270**, P. 128629.
- [26] Bhushan B., Gopinath P. Antioxidant nanozyme: a facile synthesis and evaluation of the reactive oxygen species scavenging potential of nanoceria encapsulated albumin nanoparticles. *J. Mater. Chem. B*, 2015, **3**(24), P. 4843–4852.
- [27] Yang Z., Luo S., Zeng Y. et al. Albumin-Mediated Biomineralization of Shape-Controllable and Biocompatible Ceria Nanomaterials. *ACS Appl. Mater. Interfaces*, 2017, **9**(8), P. 6839–6848.
- [28] Yeni Y., Genc S., Nadaroglu H. et al. Effects of quercetin-immobilized albumin cerium oxide nanoparticles on glutamate toxicity: in vitro study. Naunyn. Schmiedebergs. Arch. Pharmacol., 2025, 398(5), P. 5147–5156.
- [29] Khoshgozaran Roudbaneh S.Z., Kahbasi S., Sohrabi M.J. et al. Albumin binding, antioxidant and antibacterial effects of cerium oxide nanoparticles. J. Mol. Liq., 2019, 296, P. 111839.
- [30] Shcherbakov A.B., Teplonogova M.A., Ivanova O.S. et al. Facile method for fabrication of surfactant-free concentrated CeO<sub>2</sub> sols. *Mater. Res. Express*, 2017, 4(5), P. 055008.
- [31] Creed S., McKenzie M. Measurement of Mitochondrial Membrane Potential with the Fluorescent Dye Tetramethylrhodamine Methyl Ester (TMRM), Methods Mol. Biol., 2019, 1928, P. 69–76.
- [32] Luik A.I., Naboka Y.N., Mogilevich S.E. et al. Study of human serum albumin structure by dynamic light scattering: two types of reactions under different pH and interaction with physiologically active compounds. Spectrochim. Acta Part A Mol. Biomol. Spectrosc., 1998, 54(10), P. 1503– 1507
- [33] Velichko E., Makarov S., Nepomnyashchaya E. et al. Molecular Aggregation in Immune System Activation Studied by Dynamic Light Scattering. *Biology* (Basel), 2020, 9(6), P. 123.
- [34] Bardik V., Gotsulskii V., Pavlov E. et al. Light scattering study of human serum albumin in pre-denaturation: Relation to dynamic transition in water at 42° C. J. Mol. Liq., 2012, 176, P. 60–64.
- [35] Liu Y., Yang Z., Zhang X. et al. Shape/Crystal Facet of Ceria Induced Well-Dispersed and Stable Au Nanoparticles for the Selective Hydrogenation of Phenylacetylene. Catal. Letters, 2019, 149(2), P. 361–372.
- [36] Filippova A.D., Sozarukova M.M., Baranchikov A.E. et al. Peroxidase-like Activity of CeO<sub>2</sub> Nanozymes: Particle Size and Chemical Environment Matter. *Molecules*, 2023, **28**(9), P. 3811.
- [37] Sozarukova M.M., Kochneva E.M., Proskurnina E.V. et al. Albumin Retains Its Transport Function after Interaction with Cerium Dioxide Nanoparticles. ACS Biomater. Sci. Eng., 2023, 9(12), P. 6759–6772.
- [38] Pustulka S.M., Ling K., Pish S.L. et al. Protein Nanoparticle Charge and Hydrophobicity Govern Protein Corona and Macrophage Uptake. ACS Appl. Mater. Interfaces, 2020, 12(43), P. 48284–48295.
- [39] Lundqvist M., Stigler J., Elia G. et al. Nanoparticle size and surface properties determine the protein corona with possible implications for biological impacts. Proc. Natl. Acad. Sci., 2008, 105(38), P. 14265–14270.
- [40] Chaudhary Y.S., Panigrahi S., Nayak S. et al. Facile synthesis of ultra-small monodisperse ceria nanocrystals at room temperature and their catalytic activity under visible light. J. Mater. Chem., 2010, 20(12), P. 2381.
- [41] Barth A. The infrared absorption of amino acid side chains. Prog. Biophys. Mol. Biol., 2000, 74(3-5), P. 141-173.
- [42] Diaconeasa Z., Barbu-Tudoran L., Coman C. et al. Cerium oxide nanoparticles and its cytotoxicity human lung cancer cells. *Rom. Biotechnol. Lett.*, 2015, **20**, P. 10679.
- [43] Tang J., Luan F., Chen X. Binding analysis of glycyrrhetinic acid to human serum albumin: Fluorescence spectroscopy, FTIR, and molecular modeling. *Bioorg. Med. Chem.*, 2006, **14**(9), P. 3210–3217.
- [44] Usoltsev D., Sitnikova V., Kajava A. et al. Systematic FTIR Spectroscopy Study of the Secondary Structure Changes in Human Serum Albumin under Various Denaturation Conditions. *Biomolecules*, 2019, **9**(8), P. 359.
- [45] Umezawa M., Itano R., Sakaguchi N. et al. Infrared spectroscopy analysis determining secondary structure change in albumin by cerium oxide nanoparticles. *Front. Toxicol.*, 2023, **5**, P. 1237819.
- [46] Kogelheide F., Kartaschew K., Strack M. et al. FTIR spectroscopy of cysteine as a ready-to-use method for the investigation of plasma-induced chemical modifications of macromolecules. *J. Phys. D. Appl. Phys.*, 2016, 49(8), P. 084004.
- [47] Patel V., Jose L., Philippot G. et al. Fluoride-assisted detection of glutathione by surface Ce<sup>3+</sup>/Ce<sup>4+</sup> engineered nanoceria. *J. Mater. Chem. B*, 2022, **10**(47), P. 9855–9868.
- [48] Proskurnina E.V., Sozarukova M.M., Ershova E.S. et al. Lipid Coating Modulates Effects of Nanoceria on Oxidative Metabolism in Human Embryonic Lung Fibroblasts: A Case of Cardiolipin. *Biomolecules*, 2025, **15**(1), P. 53.
- [49] Yuan D., Shen Z., Liu R. et al. Study on the binding of cerium to bovine serum albumin. J. Biochem. Mol. Toxicol., 2011, 25(4), P. 263–268.
- [50] Simón-Vázquez R., Lozano-Fernández T., Peleteiro-Olmedo M. et al. Conformational changes in human plasma proteins induced by metal oxide nanoparticles. *Colloids Surfaces B Biointerfaces*, 2014, 113, P. 198–206.
- [51] Liu W., Rose J., Plantevin S. et al. Protein corona formation for nanomaterials and proteins of a similar size: hard or soft corona? *Nanoscale*, 2013, 5(4), P. 1658.
- [52] Sozarukova M.M., Proskurnina E.V., Baranchikov A.E. et al. Antioxidant Activity of Conjugates of Cerium Dioxide Nanoparticles with Human Serum Albumin Isolated from Biological Fluids. *Russ. J. Inorg. Chem.*, 2023, **68**(10), P. 1495–1502.

Submitted 8 October 2025; accepted 15 October 2025

*Information about the authors:* 

*Elena V. Proskurnina* – Kurnakov Institute of General and Inorganic Chemistry of the Russian Academy of Sciences, Moscow 119991, Russia; ORCID 0000-0002-8243-6339; proskurnina@gmail.com

Svetlana V. Kostyuk – Kurnakov Institute of General and Inorganic Chemistry of the Russian Academy of Sciences, Moscow 119991, Russia; Petrovsky Russian Scientific Center of Surgery, Institute of Longevity with a Clinic of Rehabilitation and Preventive Medicine, Moscow 119435, Russia; ORCID 0000-0002-6336-9900; svet-vk@yandex.ru

*Madina M. Sozarukova* – Kurnakov Institute of General and Inorganic Chemistry of the Russian Academy of Sciences, Moscow 119991, Russia; ORCID 0000-0002-5868-4746; s\_madinam@bk.ru

*Elizaveta S. Ershova* – Kurnakov Institute of General and Inorganic Chemistry of the Russian Academy of Sciences, Moscow 119991, Russia; Petrovsky Russian Scientific Center of Surgery, Institute of Longevity with a Clinic of Rehabilitation and Preventive Medicine, Moscow 119435, Russia; ORCID 0000-0003-1206-5832; es-ershova@rambler.ru

*Natalia N. Veiko* – Kurnakov Institute of General and Inorganic Chemistry of the Russian Academy of Sciences, Moscow 119991, Russia; Petrovsky Russian Scientific Center of Surgery, Institute of Longevity with a Clinic of Rehabilitation and Preventive Medicine, Moscow 119435, Russia; ORCID 0000-0003-1847-0548; satelit32006@yandex.ru

*Matvei A. Popkov* – Kurnakov Institute of General and Inorganic Chemistry of the Russian Academy of Sciences, Moscow 119991, Russia; ORCID 0000-0002-9811-6241; ma\_popkov@igic.ras.ru

Edmund V. Kostyuk – Kurnakov Institute of General and Inorganic Chemistry of the Russian Academy of Sciences, Moscow 119991, Russia; ORCID 0000-0001-7033-6843; edmundvk@ya.ru

Andrey V. Martynov – Kurnakov Institute of General and Inorganic Chemistry of the Russian Academy of Sciences, Moscow 119991, Russia; ORCID 0000-0002-6697-8306; avlamar@mail.ru

Vladimir K. Ivanov – Kurnakov Institute of General and Inorganic Chemistry of the Russian Academy of Sciences, Moscow 119991, Russia; ORCID 0000-0003-2343-2140; van@igic.ras.ru

Conflict of interest: the authors declare no conflict of interest.